HYDRATION OF A CLAY-RICH UNIT ON MARS, COMPARISON OF ORBITAL SPECTRAL DATA TO ROVER NEUTRON RESULTS. S. Czarnecki[1], C. Hardgrove[1], R. E. Arvidson[2], M. N. Hughes[2], M. E. Schmidt[3], T. Henley[3], L. M. Martinez Sierra[4], I. Jun[4], T. Gabriel[5], M. Litvak[6], I. Mitrofanov[6], [1]Arizona State Univ., sean.czarnecki@asu.edu, [2]Washington Univ. St. Louis, [3]Brock Univ., [4]Jet Propulsion Lab, [5]USGS, [6]Space Research Inst., RAS.

Introduction: The Mars Science Laboratory (MSL) Curiosity rover recently conducted detailed investigations of the chemistry, mineralogy, and hydration of an area known as Glen Torridon (GT), on the slopes of Mt. Sharp in Gale crater. Data from the Mars Reconnaissance Orbiter's (MRO) Compact Reconnaissance Imaging Spectrometer for Mars (CRISM) instrument [1] were used to detect the presence of ferric smectites in GT [2,3], and data from the MSL CheMin instrument showed that GT bedrock drill samples contain abundant smectite minerals (most samples between 28-34 wt.%) [4].

Both the CRISM and MSL Dynamic Albedo of Neutrons (DAN) instruments are sensitive to hydration, but DAN measurement locations are limited to the relatively small fraction of GT through which Curiosity traversed, whereas the CRISM data cover the entire GT region. Additionally, the DAN sensing volume (bulk rock within a few m surface footprint to a depth of tens of cm) is significantly different than the CRISM sensing volume (pixels tens of m wide and several µm deep). Here, we compare DAN and CRISM hydration results in GT to understand the bulk hydration of this clay-rich unit and to explore the effects that surface cover and texture have on these comparisons.

DAN: DAN is a neutron spectrometer with a pulsed neutron generator (PNG) and two He-3 neutron detectors [5]. In active mode, the DAN PNG produces 14.1 MeV neutron pulses at 10 Hz. A typical measurement lasts 20 minutes, during which neutrons are isotropically emitted with each pulse. A fraction of these neutrons enter the martian subsurface, interact with subsurface nuclei, and return to the detectors. Neutron counts are recorded between each pulse in lognormal time bins and the counts in each time bin are summed for all pulses. A plot of neutron counts as a function of time after pulse is known as a `die-away' curve, whose shape is dependent on the depth and abundance of neutron scatterers (primarily hydrogen) and thermal neutron absorbers (e.g., iron, chlorine) [6].

We subtracted background neutron count rates and compared DAN data to simulation data produced using the MCNP6 code [7], which simulates neutron transport in a 3D environment. Our simulations each include a model rover, atmosphere, and subsurface composition. In this study, each subsurface model is laterally and vertically homogeneous. We used a grid of subsurface compositions with variable bulk water-equivalent hydrogen (WEH, a standard quantity used to report the hydrogen abundance as an equivalent water abundance) and thermal neutron absorption cross section Σ_{abs} (a measure of the probability of a thermal neutron being absorbed). WEH and Σ_{abs} were varied across the range of values measured in Gale crater. To determine the WEH and Σ_{abs} for each DAN active measurement, we compared the DAN die-away curves to the grid of simulated die-away curves using a Markov-chain Monte Carlo (MCMC) analysis method as in [8]. We used the MCMC results to derive mean values and uncertainties for the variable parameters (WEH and Σ_{abs}).

CRISM: We chose to use an along-track oversampled CRISM observation (FRT00021C92) centered over GT. This allowed projection at 12 m/px using a log maximum likelihood approach for surface reflectance retrieval and regularization as described in [9]. The DISORT radiative code was used to model atmospheric contributions and the Hapke surface photometric function [10] simulated incidence, emergence, and phase angle effects on the surface single scattering albedo (SSA) for each pixel [11]. Thermal emission from the surface and atmosphere were also included. Data were processed using a neural network approach [9] to solve the undetermined nature of retrieving surface SSA for wavelengths longer than ~2.65 µm. We used a 3 µm integrated band index (BDI) for comparison to DAN WEH results. This index is associated with the 3 µm H_2O symmetrical and asymmetrical stretch absorptions, the 6.0 H_2O fundamental bending mode absorption overtone, and the OH fundamental stretch absorption [12]. The 3 µm BDI was generated by calculating a continuum spectrum between 2.1-3.7 µm and then computing the area under the continuum spectrum between 2.9-3.7 µm, using the actual widths of relevant spectral bands.

We registered the projected CRISM scene to a MRO HiRISE mosaic used by the MSL team for localization [13]. To mitigate imperfect registration, the CRISM data were resampled to 24 m/px. Where necessary, we computed the mean DAN WEH for all DAN measurements within a CRISM pixel. We determined sand cover fraction using the HiRISE basemap in ArcGIS and removed pixels with > 10% sand cover.

Results/Discussion: The Table lists the mean DAN WEH for GT and adjacent Vera Rubin ridge (VRR) units. GT units have higher mean WEH (3.7-4.1 wt.%) while the VRR units have lower mean WEH (3.1 wt.%).

Geologic Unit	# DAN Sites	Mean WEH [wt.%]	Std. Dev. [wt.%]
PPm/VRR	26	3.1 ± 0.7	0.6
Jm/VRR	19	3.1 ± 0.7	0.7
Jm/GT	29	4.0 ± 0.8	0.6
KHm/GT	19	4.1 ± 0.7	0.5
Gm/GT	26	3.7 ± 0.9	0.9
Sf/GP	2	2.7 ± 0.8	1.4

Table 1: DAN Results. Mean WEH includes the mean WEH uncertainty. PPm = Pettegrove Point, Jm = Jura, KHm = Knockfarril Hill, Gm = Glasgow, Sf = Stimson.

A comparison of DAN WEH vs. CRISM 3 µm BDI suggests that units with rough surface textures have enhanced 3 µm absorption compared to units with similar bulk WEH but smooth surface textures. We classified the surface texture of each CRISM pixel within the study area as either `regolith' (rough) or `bedrock' (smooth), using descriptions of geomorphic units in GT mapped by [14], and based on inspection of the HiRISE mosaic for VRR units.

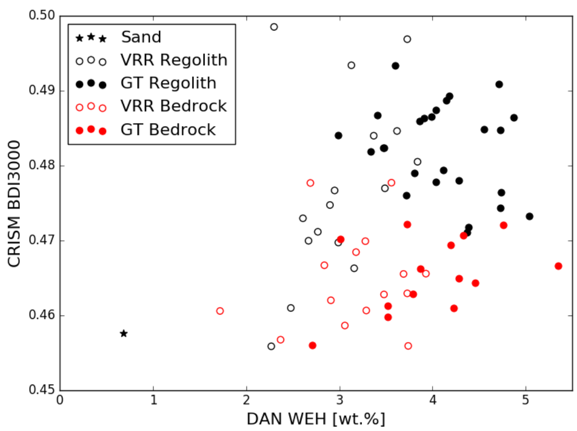

Figure 1: Plot of DAN WEH vs. CRISM 3 µm BDI classified by surface texture and geomorphic feature (VRR or GT). A low-WEH data point from a previous sand dune measurement [8] is included for reference.

In Figure 1, GT data points (filled circles) have higher WEH values than VRR data points (hollow circles). This is also shown by the mean values of associated units in the Table. GT is among the most hydrated intervals along the MSL traverse, which correlates with the relatively large clay abundances measured by CheMin in GT compared to most previous stratigraphic units. While more work needs to be done in order to determine the specific subsurface distribution of water in GT, the colocation of clay-rich samples in water-rich units suggests that clay minerals could be a significant subsurface water reservoir.

There is a clear enhancement of CRISM 3 µm BDI for regolith (black) compared to bedrock (red) in both VRR and GT, though this is more distinct for GT. This shows that surface texture exerts a strong control on the CRISM 3 µm BDI. DAN measurements are insensitive to surface texture, and the mean WEH for regolith material in the study area is the same as that for bedrock material (both are 3.6 ± 0.8 wt.% WEH).

Given the significant effect that surface texture has on CRISM results and the granularity of a two-category classification scheme for surface texture, it is not surprising that these data sets do not show a strong linear correlation. However, both the regolith and bedrock data sets shown in Figure 1 are consistent with loose positive correlations between CRISM 3 µm BDI and DAN WEH. Future studies utilizing this spectral feature must account for differences in surface texture and the abundance of surface cover like sand. For areas of predominantly exposed bedrock, CRISM 3 µm integrated band depth results are representative of the relative bulk hydration at the pixel scale (tens of meters). At the smaller scale of a few meters, DAN measurements can be used to identify locations with enhanced hydration (potentially due to clay minerals) and provide absolute WEH abundances independent of surface texture.

Acknowledgments: The authors wish to thank Patrick Gasda, Kathryn Powell, Scott VanBommel, and Daniel Sullivan for helpful conversations. Support was provided by the MSL Participating Scientist Program. All data used are available on the NASA PDS.
pds-geosciences.wustl.edu/missions/msl/dan.htm
pds-imaging.jpl.nasa.gov/volumes/msl.html
pds-geosciences.wustl.edu/missions/mro/crism.htm

References: [1] Murchie, S., et al. (2007) *JGR:P, 112*(5), 1-57. [2] Millikan, R. E., et al. (2010) *GRL, 37*, L04201. [3] Fraeman, A. A., et al. (2016) *JGR:P, 121*, 1713-1736. [4] Thorpe, M. T., et al. (2021) *JGR:P, submitted*. [5] Mitrofanov, I. G., et al. (2012) *Space Sci. Rev., 170*, 559-582. [6] Hardgrove, C., et al. (2011) *NIMA, 659*, 442-455. [7] Werner, C. J., et al. (2018) MCNP user's manual: Code version 6.2. LA-UR-17-29981. [8] Gabriel, T. S. J. et al. (2018) *GRL, 45*. [9] He, L., et al. (2021) *JGR:P, submitted*. [10] Hapke, B. R. (2012) Theory of Reflectance and Emittance Spectroscopy, *Cambridge Univ. Press, 2nd ed.* [11] Arvidson, R. E. et al., (2015) *JGR:P, 120*, 429-451. [12] Rossman, G. R. (1988) Spectroscopic Methods in Mineralogy and Geology, *Min. Soc. Amer., 18*, Ch. 6. [13] Calef III, F., et al. (2016) MSL Gale merged orthophoto mosaic. PDS Anne, US Geo. Surv. [14] Hughes, M.N., et al. (2021) *JGR:P, submitted*.